OTIMIZAÇÃO DA ESPESSURA DO PAVIO EM UM TUBO DE CALOR DE PLACA PLANA COM MÚLTIPLAS FONTES DE CALOR

OPTIMIZATION OF THE WICK THICKNESS IN A FLAT PLATE HEAT PIPE WITH MULTIPLE HEAT SOURCES

ОПТИМИЗАЦИЯ ТОЛЩИНЫ ФИТИЛЯ В ПЛОСКОЙ ПЛАСТИНЧАТОЙ ТЕПЛОВОЙ ТРУБЕ С НЕСКОЛЬКИМИ ИСТОЧНИКАМИ ТЕПЛА

RABINSKIY, Lev N.[1*]; POLYAKOV, Pavel O.[1]; SOLYAEV, Yury O.[1,2]

[1] Moscow Aviation Institute (National Research University), 4 Volokolamskoe shosse, zip code 125993, Moscow – Russian Federation
(phone: +7 499 158-43-33)

[2] Institute of Applied Mechanics of Russian Academy of Sciences, 7 Leningradsky Ave., zip code 125040, Moscow – Russian Federation
(phone: +7 495 946-18-03)

** Corresponding author*
e-mail: rabinskiy@mail.ru

Received 2 June 2018; received in revised form 21 November 2018; accepted 05 December 2018

RESUMO

Com base em modelos bidimensionais simplificados de calor e hidrodinâmica, os autores estimaram a espessura ótima da camada do pavio, que deve ser sinterizado dentro do tubo de calor com placa plana para garantir seu máximo desempenho, a saber: limite capilar alto e baixa temperatura do microelemento resfriado. O modelo usa as paredes externas do tubo de calor, que são consideradas como as condições de convecção não-adiabáticas e livres. As suposições sobre o fluxo de gás laminar no núcleo de vapor e o modelo de Darcy para o fluxo de líquido no pavio são usadas. É mostrado que um máximo forte de transferência de calor de um tubo de calor pode ser conseguido escolhendo a espessura óptima da camada do pavio. A possibilidade de reduzir completamente a espessura do tubo de calor para propriedades fixas e microestrutura do pavio também está sendo estudada.

Palavras-chave: *tubo liso lamelar, pavio poroso, limite capilar, sistemas de refrigeração, transferência de calor e massa.*

ABSTRACT

Based on the simplified two-dimensional heat and hydrodynamics models we estimate an optimal thickness of the wick layer that should be sintered inside the flat plate heat pipe to provide its maximum operating performance, namely, high capillary limit and low temperature of cooled microelectronic components. External walls of the heat pipe assumed to be non-adiabatic and free convection conditions are used in the model. Assumptions of laminar gas flow in the vapor core and Darcy's model for liquid flow in the wick are utilized. It is shown that a strong maximum of the heat pipe total heat transfer capability can be achieved by choosing the optimal value of the wick layer thickness. The possibility of the heat pipe total thickness reduction is also investigated for fixed properties and microstructure of the wick.

Keywords: *flat plate heat pipe, porous wick, capillary limit, cooling systems, heat and mass transfer.*

DOI: 10.52571/PTQ.SI1.2018.450_PeriodicoES.pdf

АННОТАЦИЯ

На основе упрощенных двумерных моделей тепловой и гидродинамики авторами оценена оптимальная толщина слоя фитиля, который должен быть спечен внутри тепловой трубы с плоской пластиной, чтобы обеспечить ее максимальные рабочие характеристики, а именно: высокий капиллярный предел и низкую температуру охлажденного микроэлемента – тронные компоненты. В модели используются наружные стенки тепловой трубки, которые считаются неадиабатическими и свободными конвекционными условиями. Используются предположения о потоке ламинарного газа в сердцевине пара и модели Дарси для потока жидкости в фитиле. Показано, что сильный максимум теплопередачи тепловой трубы может быть достигнут путем выбора оптимального значения толщины слоя фитиля. Также изучается возможность полного уменьшения толщины тепловой трубы для фиксированных свойств и микроструктуры фитиля.

Ключевые слова: *плоская пластинчатая труба, пористый фитиль, капиллярный предел, системы охлаждения, тепломассоперенос.*

INTRODUCTION

Flat plate heat pipes (FPHP) are widely studied in recent years due to its high capillary limit and low thickness that allow to use it in various cooling systems of electronic devices even when a very little space is alFPHP's and vapor chambers were started more than twenty years ago (Vafai and Wang, 1992; Huang and Liu, 1996; Ooijen and Hoogendoorn, 1979), however its wide application and experimental and theoretical investigation were intensively performed in a recent decade (Chen and Chou, 2014; Blet *et al.*, 2017; Weibel and Garimella, 2013; Faghri, 2014; Lee and Byon, 2018; Lv and Li, 2017).

Present paper deals with the theoretical modeling of the FPHP that could be used in the high-power transmitting/receiving electronic devices (Formalev and Kolesnik, 2018; Formalev *et al.*, 2016). Multiple heat sources (microchips) are maintained and provided an input heat flux at the one end of the heat pipe, while the condenser region is placed at the other end. The goal of the simulations is to find a possible thinnest variant of the FPHP that allows transferring the heat from the evaporator area to condenser without an overheating of the microchips and without achieving the capillary limit of FPHP.

In our studies, we use the simplified variant of the steady-state model that was proposed initially in (Lefèvre and Lallemand, 2006) and studied later in (Lips and Lefevre, 2014). In this model, the 3D heat model of the FPHP walls together with 2D hydrodynamic models for the vapor core and liquid saturated wick are used. Isothermal laminar flow conditions for the vapor core are assumed (Zuas, 2017; Luo *et al.*, 2005). A considered approach is extended now for the transient processes and more complex physical models of the gas/liquid flow (Revellin *et al.*, 2009; Sonan *et al.*, 2008; Hassan and Harmand, 2013; Bejan, 2013).

In the present paper, we simplified the initial variant of the model (Lefèvre and Lallemand, 2006) by using the 2D thermal model under the assumption of the small thickness of the FPHP walls. However, we add an extra term in the heat transfer model to take into account non-adiabatic conditions on the external walls of the heat pipe, that is related with free convection that is usually realized in considered systems.

MATERIALS AND METHODS

The authors consider FPHP of rectangular shape with dimensions $a \times b$ in XY plane; its total thickness in the z-direction is H. Multiple heat sources of different power and single condenser are placed at the one side of FPHP. Domain occupied by the FPHP in XY plane will be denoted as Ω and its boundary is $\partial\Omega$. Solid walls have constant thickness H_s. Thicknesses of the wick and of the vapor core are denoted as H_l and H_v, respectively.

Operating processes in considered heat pipe are the following. Heat is applied at the evaporator region, where the multiple heat sources are placed, and removed at the condenser, where the external liquid or air cooling system is used. The fluid vaporized around the evaporator region due to input heat. The arisen vapor pressure drives the vapor from the evaporator to the condenser, where the vapor condenses to a liquid. The capillary pressure in the wick provides the liquid backflow to the evaporator.

All processes are assumed to be steady state and two-dimensional due to small thicknesses of the wall, wick and vapor core. Uniform temperature (equal to the saturation temperature T_{sat}) and laminar flow are assumed for the vapor core. Darcy's model is used for the liquid flow in the wick which is isotropic and completely saturated. Liquid and vapor flows are assumed to be incompressible. Condensation/evaporation are realized only at the interface between the vapor and liquid-wick.

Based on made assumptions we can propose the following statement of the heat and mass transfer models (Lefèvre and Lallemand, 2006). Heat conduction equation for the heat transfer in solid walls (Equation 1), where T is the temperature of the FPHP wall; ∇ is 2D nabla operator; k_s is thermal conductivity of the wall; **n** is the unit normal vector to the domain's boundary; φ is given input/output heat flux that is prescribed at the evaporator and condenser area, $\varphi_0 = h_0(T_0 - T)$ is an output heat flux from the FPHP walls to the outer space due to free convection; h_0 is the heat transfer coefficient between walls and outer space, which temperature is T_0. Mass balance equation and Darcy's low for the liquid flow in the porous wick (Equation 2), where ρ_l, μ_l and K are density, dynamic viscosity and permeability of the liquid; $\boldsymbol{u}_l$ is the liquid velocity field; P_l is pressure in the liquid; $\rho_l \boldsymbol{g}$ is gravitational force; $\alpha = h(T-T_{sat})/L_v$ is evaporation rate that is evaluated as the ratio of heat flux coming from the wall to the latent heat of vaporization L_v; $h = k_s / H_l$ is heat transfer coefficient between wall and vapor core, k_l is thermal conductivity of the liquid saturated wick. Finally, the mass balance equation and velocity field for the vapor is derived based on the model of the laminar incompressible two-dimensional flow between two parallel plates (Lefèvre and Lallemand, 2006; Bejan, 2013) (Equation 3), where ρ_V and μ_V are density and dynamic viscosity of the vapor; $\boldsymbol{u}_V$ is the vapor velocity field; P_V is pressure in the vapor.

Presented models (Equations 1 – 3) were implemented in Comsol and solved by using its standard FE solver. Quadrilateral mesh with second-order elements was used. A total number of the elements in the model was about 5000. One can see that considered problem (Equations 1 – 3) consist of three coupled Poisson-type equations with Neumann-type boundary conditions. Solutions of these PDE's give us the functions of temperature T, liquid pressure P_l and vapor pressure P_v that are unique up to some constants T_0, P_{l0}, P_{v0}. These constants are set to be equal to the predefined saturation temperature of the water vapor $T_0 = T_{sat}$ and its corresponding saturation pressure $P_{l0} = P_{v0} = P_{sat}$ under the steady-state regime of the FPHP operation.

RESULTS AND DISCUSSION:

The authors consider flat heat pipe with dimensions 400×200 mm and with wall thickness, H_S = 0.5 mm. Scheme of considered FPHP and power of heat sources are given in Figure 1. The material of the walls and wick is copper. The thermal conductivity of the walls is 380 W/(m K). The effective thermal conductivity of the liquid saturated wick is 1.5 W/(m K). Heat transfer coefficient between FPHP and outer space is h_0 = 5 W/(m^{2}K), ambient temperature is T_0 = 22 °C. Working fluid is water, which latent heat of evaporation is L_V = 2260 kJ/m^3. The permeability of the wick is $K = 1 \cdot 10^{-11}$ m^2. Dynamic viscosities and densities of liquid and vapor are μ_l = 0.001Pa m, $\mu_V = 10^{-5}$Pa m, ρ_l = 990 kg/m^3, ρ_V = 0.017 kg/m^3. Surface tension in the wick pores is σ = 0.1 N/m and effective pores radius is r_{eff} = 50 μm, therefore the capillary limit of FHP can be approximately defined by $\Delta P_C = 2\ \sigma / r_{eff}$ = 4000 Pa. Saturation temperature is set to be T_{sat} = 50°C and corresponding saturation pressure is P_{sat} = 12.3 KPa. Anti-gravitation regimes of FPHP operation is considered.

Example of the simulation results for the FPHP with total thickness H = 3 mm and with wick thickness H_l = 0.5 mm are presented in Figure 2. Power of the heat sources is defined by the value Q_0 = 10 W. Maximum velocity of the vapor flow is about 22 m/s that is much higher than the liquid velocity in the wick, which is about 0.7 mm/s (Figure 2a). Pressure drop in the liquid phase is ΔP_l = 3540 Pa and in the vapor phase, ΔP_v = 60 Pa (Figure 2b). The maximum temperature of the FPHP surface at the evaporator region is T_{max} = 56 °C (Figure 2c). Maximum heat transport capability of the FPHP is defined by the value of the heat sources total power $Q = 4.8Q_{max}$ that leads to the equality between the total pressure drop and the capillary pressure: $\Delta P_l + \Delta P_v = \Delta P_c$. For the considered type of FPHP (Figure 1) it is found that Q = 54 W. Corresponding maximum temperature of the FPHP surface will be T_{max} = 57 °C in this limiting case.

Next, we estimate the dependence of the FPHP maximum performance Q and corresponding maximum temperature T_{max} for different values of the wick and vapor core thicknesses. The results are presented in Figure 3. It is found that and the optimal value of the wick thickness is existed and allows to obtain the maximum heat transfer capability of FPHP. This maximum arises due to the opposite effects that are realized when we increase the wick thickness – the pressure drop in the liquid phase is decreased while the pressure drop in the vapor is increased. The optimal thickness of the wick corresponds to the minimum total pressure drop in the wick and vapor flow for given properties of the fluid and microstructure (that define the permeability) of the wick. The maximum temperature of FPHP is higher for larger values of the wick thickness due to the decrease of the heat transfer coefficient *h* between walls and vapor core (Figure 3b). Maximum temperature does not depend on the vapor core thickness in the considered model due to the assumption of two-dimensional isothermal vapor flow.

From Figure 3 it follows that for a given total thickness of the FPHP, that could be limited by the design requirements and restrictions of the considered electronic system, it could be found an optimal value of the wick thickness and optimal performance of the heat pipe can be achieved. Maximum temperature does not significantly increase and remain less than the 70 degrees that are usually acceptable for the considered type of electronic systems. Dependence of maximum possible heat transfer capability for a given total thickness of FPHP is presented in Figure 4. The result of such type can be useful for the preliminary design of an electronic system: one can see the maximum performance of considered FPHP under given restrictions of its total thickness. If the possible thickness of FPHP should be not more than H = 3 mm, than the FPHP performance can be improved up to Q = 210 W, while if we have H = 2 mm than we will achieve not more than Q = 75 W.

Additional reduction of the FPHP thickness without loss of its heat transfer capability can be realized only if we will use the thinner solid walls, however, it cannot be acceptable in some cases due to loss of the mechanical stiffness.

CONCLUSIONS:

In this paper, the authors present the results of the FPHP optimization by considering only the wick thickness as the variable. Values of the maximum performance and maximum heat transfer capability of FPHP are estimated by using numerical finite-element simulations. It is shown that a strong maximum of the FPHP performance can be obtained by choosing an optimal value of the wick thickness. For example, for considered copper/water FPHP with multiple sources and with a total thickness of 2 mm the optimal value of the wick thickness will be about 0.7 mm. This rather high value of the wick thickness leads to the increase of the FPHP temperature in 5-6 degrees (in comparison with FPHP with smallest wick's thickness of 0.1-0.2 mm), however, it remains lower than the maximum allowable operating temperature of electronic components in considered devices. Dependence of the FPHP possible maximum performance that can be achieved for given total thickness is also obtained.

Presented results are obtained by using simplified two-dimensional steady-state thermal/hydrodynamic model. This model can be useful for the preliminary design of FPHP and cooling systems of electronic devices, however, the more general analysis should be involved for accurate predictions of the FPHP performance, including 3D transient analysis with more precise geometry representation. Namely, in the present work, we neglect the effects of the wick columns that are usually sintered inside the FPHP to provide its stiffness under transversal compression. Additionally, another type of the FPHP limits should be considered during precise analyses, e.g., sonic and entrainment limits related with the vapor flow velocity should be checked.

ACKNOWLEDGMENTS:

The work was supported by the Russian Ministry of Science and Education (Contract No 14.574.21.0166, RFMEFI57417X0166).

REFERENCES:

1. Bejan, A. *Convection heat transfer*. Hoboken: John Wiley & Sons, **2013**.

2. Blet, N., Lips, S., Sartre, V. *Applied Thermal Engineering*, **2017**, *118*, 490–509.

3. Buch, A. *Engineering Studies*, **2016**, *8(2)*, 140-161.

4. Chen, J.-S., Chou, J.-H. *International Journal of Heat and Mass Transfer*, **2014**, *77,* 874-882.

5. Faghri, A. *Frontiers in Heat Pipes (FHP),* **2014**, *5(1)*. Available at: https://ru.scribd.com/document/323642833/HEAT-PIPES-Review-Opportunities-and-Challenges

6. Formalev, V.F., Kolesnik, S.A. *International Journal of Heat and Mass Transfer*, **2018**, *123*, 994-998.

7. Formalev, V.F., Kolesnik, S.A., Kuznetsova, E.L., Rabinskiy, L.N. *International Journal of Pure and Applied Mathematics*, **2016**, *111(2)*, 303-318.

8. Hassan, H., Harmand, S. A *Heat Transfer Engineering*, **2013**, *34(7)*, 596-607.

9. Hassan, H., Harmand, S. *Journal of Heat Transfer*, **2013**, *135 (11)*, 111008.

10. Huang, X.Y., Liu, C.Y. *International Journal of Heat and Mass Transfer*, **1996**, *39(6)*, 1325-1330.

11. Lee, D., Byon, C. *International Journal of Heat and Mass Transfer*, **2018**, *122*, 306-314.

12. Lefèvre, F., Lallemand, M. *International Journal of Heat and Mass Transfer*, **2006**, *49(7-8)*, 1375-1383.

13. Lips, S., Lefevre, F. *International Journal of Heat and Mass Transfer*, **2014**, *72 (2014)*, 288-298.

14. Luo, Q.-H., Tang, G.-F., Li, N.-P. *Journal of Asian Architecture and Building Engineering*, **2005**, *4(1)*, 217-222.

15. Lv, L., Li, J. *Applied Thermal Engineering*, **2017**, *122*, 593-600.

16. Ooijen, H. van, Hoogendoorn, C.J. *AIAA Journal*, **1979**, *17(11)*, 1251-1259.

17. Revellin, R., Rullie`re, R., Lefe`vre, F. Bonjour, J. *Applied Thermal Engineering*, **2009**, *29*, 1114-1122.

18. Sonan, R., Harmand, S., Pell´e, J., Leger, D., Fak`es, M. *International Journal of Heat and Mass Transfer*, **2008**, *51 (25-26)*, 6006-6017.

19. Vafai, K., Wang, W. *International Journal of Heat and Mass Transfer*, **1992**, *35(9)*, 2087-2099.

20. Weibel, J.A., Garimella, S.V. *Advances in Heat Transfer*, **2013**, *45*, 209-301.

21. Zuas, O. *Periodico Tche Quimica*, **2017**, *14(28)*, 120-129.

$$k_s H_s \nabla^2 T = \phi + h(T - T_{sat}) \quad in \quad \Omega$$
$$\nabla T \cdot \boldsymbol{n} = 0 \quad on \quad \partial\Omega \tag{1}$$

$$p_l \nabla \cdot (H_l \boldsymbol{u}_l) = -a \quad in \quad \Omega$$
$$\boldsymbol{u}_l = -\frac{K}{\mu_l}(\nabla P_l - p_l g) \quad in \quad \Omega \tag{2}$$
$$\boldsymbol{u}_l \cdot \boldsymbol{n} = 0 \quad on \quad \partial\Omega$$

$$p_v \nabla \cdot (H_v \boldsymbol{u}_v) = a \quad in \quad \Omega$$
$$\boldsymbol{u}_v = -\frac{12 H_v^2}{\mu_l} \nabla P_v \quad in \quad \Omega \tag{3}$$
$$\boldsymbol{u}_v \cdot \boldsymbol{n} = 0 \quad on \quad \partial\Omega$$

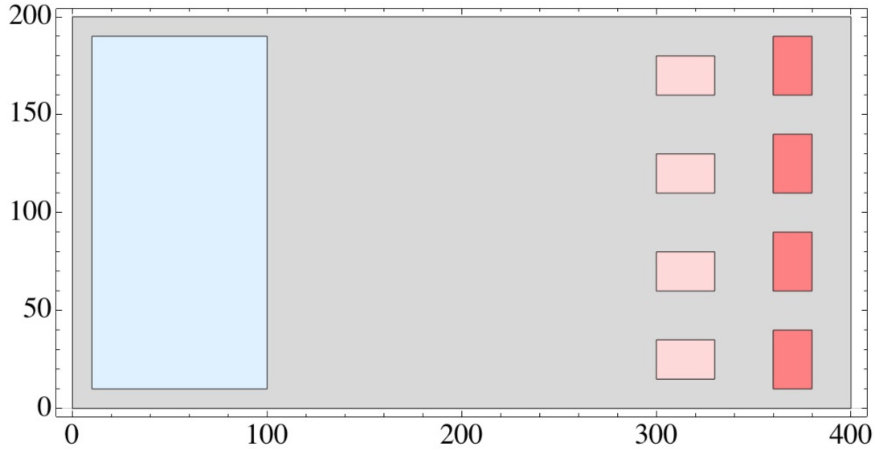

Figure 1. *Scheme of the flat plate heat pipe with multiple sources. Blue zone – condenser, red zones – main heat sources (each of the power Q_0), light red zones – additional heat sources (each of the power $Q_0/5$)*

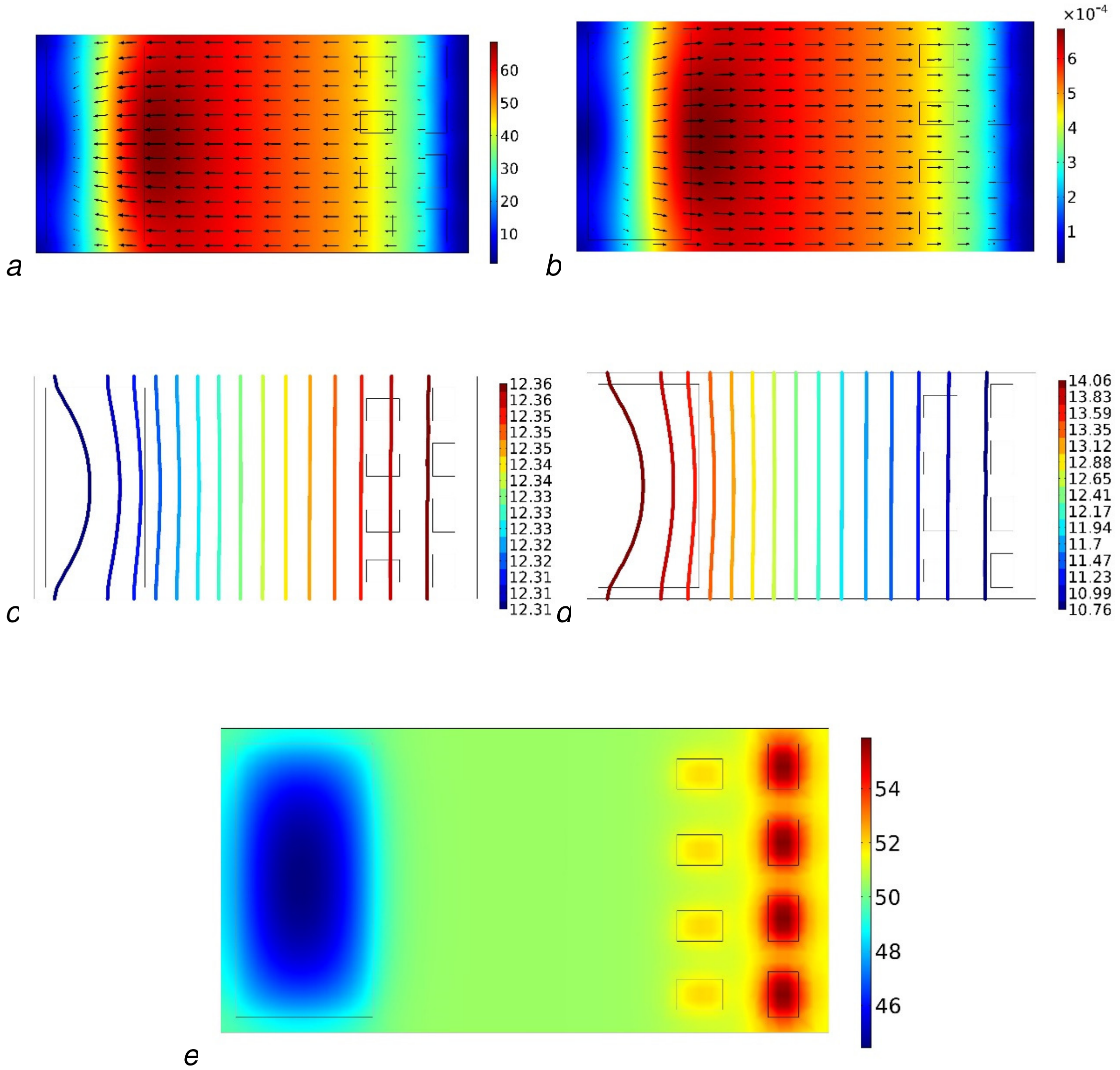

Figure 2. *Example of simulation results for the FPHP with total thickness H = 3 mm and with wick thickness H_l = 0.5 mm. Power of the heat sources is defined by Q_0 = 10 W. a: Vapor velocity field, m/s, b: Liquid velocity field, m/s, c: Pressure in liquid, KPa, d: Pressure in vapor, KPa, e: Temperature distribution over the FPHP external wall, °C*

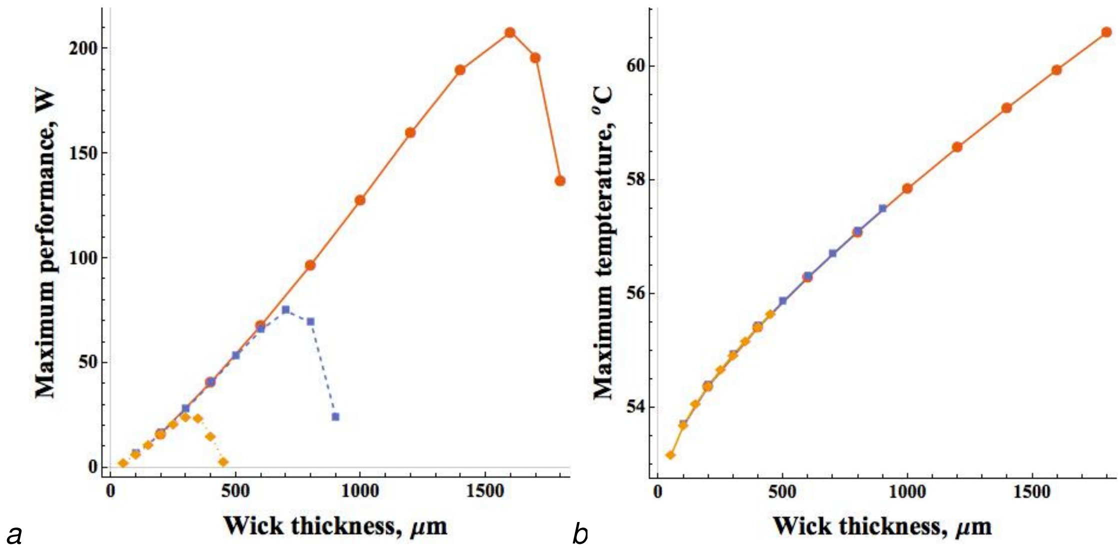

Figure 3. *Dependence of the FPHP maximum heat transfer capability (a) and maximum temperature (b) on the wick thickness and on the total thickness of FPHP: H = 2 mm (solid red line), H = 1 mm (dashed blue line), H = 0.5 mm (dotted yellow line)*

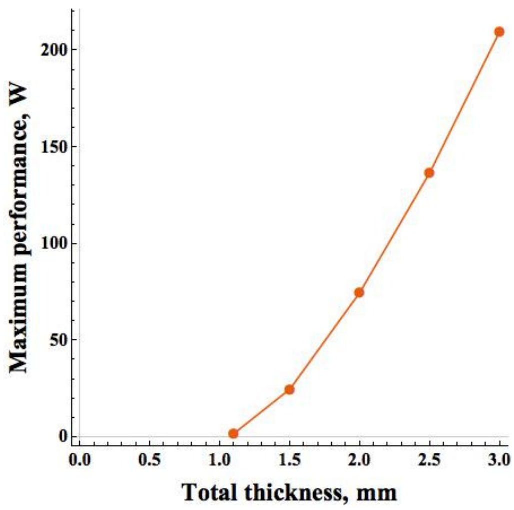

Figure 4. *Maximum possible heat transfer capability of FPHP that could be obtained by using the optimal thickness of the wick for different values of total thickness*